

# Binding Energies of the Silver Ion to Small Oxygen-Containing Ligands: Determination by Means of Density Functional Theory and Threshold Collision-Induced Dissociation

Houssain El Aribi, Tamer Shoeib, Yun Ling, Christopher F. Rodriquez, Alan C. Hopkinson, and K. W. Michael Siu\*

Department of Chemistry and Centre for Research in Mass Spectrometry, York University, 4700 Keele Street, Toronto, Ontario, Canada M3J 1P3

Received: October 31, 2001; In Final Form: January 15, 2002

The binding enthalpies at 0 K of the silver ion to water, methanol, ethanol, diethyl ether, and acetone were calculated using density functional theory (DFT) using the hybrid B3LYP level of theory with the DZVP basis set; they were also measured using the threshold collision-induced dissociation (CID) method. There is good agreement between the two sets of data. For the five ligands, the DFT/threshold CID values are: water, 28.1/31.6 ± 2.5; methanol, 30.1/33.0 ± 3.7; ethanol, 32.0/33.9 ± 3.5; diethyl ether, 33.3/33.2 ± 1.5; and acetone, 36.2/38.0 ± 1.4 kcal/mol. The average of the absolute differences between the DFT and threshold CID results is 2.0 kcal/mol, a value smaller than the average experimental uncertainty of 2.5 kcal/mol. For identical ligands, the silver ion binding energies are lower than the lithium ion binding energies, but higher than the sodium ion binding energies.

## Introduction

The bio-inorganic chemistry of the silver ion is diverse and interesting. The Ag<sup>+</sup> ion has long been used as a bactericide in eye drops for newborns.<sup>1,2</sup> Furthermore, some silver complexes have been found to have remarkable antimicrobial activities.<sup>3,4</sup> The metallothioneins, a class of small proteins believed to be involved in metal detoxification in mammals, exhibit very high affinities for Ag<sup>+</sup>.<sup>5,7</sup> Binding of Ag<sup>+</sup> to other proteins and peptides has also been observed,<sup>8–10</sup> and has been used as a means for gas-phase sequencing of peptides.<sup>11</sup>

There has been very little work on the strength of the silver-ligand bond in the gas phase for even the simplest ligands. The binding energy between Ag<sup>+</sup> and a ligand, L, is the enthalpy change, ΔH<sup>o</sup><sub>T</sub>, of the following dissociation reaction at temperature *T*, typically 0 K



The earliest quantitative study of Ag<sup>+</sup> complexes in the gas phase was for Ag(H<sub>2</sub>O)<sub>*n*</sub><sup>+</sup> (where *n* = 1–6) and for Ag(NH<sub>3</sub>)<sub>*n*</sub><sup>+</sup> (where *n* = 2–5) using high-pressure mass spectrometry.<sup>12</sup> Subsequently, the energies for formation of the diadducts, AgL<sub>2</sub>, where L = water, primary alcohols, alkyl bromides, benzene, methyl acetate, alkyl ketones, ammonia, methyl cyanide, dimethyl sulfide, and dimethyl sulfoxide, were measured via exchange equilibria in a modified atmospheric pressure ionization mass spectrometer.<sup>13</sup> The binding energies of Ag<sup>+</sup> to benzene, acetone, isoprene and 2-pentene were measured from analysis of radiative association kinetics in a Fourier transform mass spectrometer; these were found to agree well with estimated values obtained from ab initio molecular orbital calculations.<sup>14</sup> Calculated binding energies of Ag<sup>+</sup> to a number of small ligands were reported.<sup>15</sup> Recently, stepwise binding energies of Ag<sup>+</sup> to ammonia in Ag(NH<sub>3</sub>)<sub>*n*</sub><sup>+</sup> (*n* = 1–8) were

reported in a principally theoretical study using density functional theory (DFT);<sup>16</sup> good agreement with published experimental data<sup>12</sup> was reported.

Here, we report the binding energies of Ag<sup>+</sup> to a number of small oxygen-containing ligands, namely water, methanol, ethanol, diethyl ether, and acetone. These, together with ammonia, serve as models for some of the functional groups in bio-macromolecules. The binding energies were obtained both theoretically using DFT molecular orbital calculations and experimentally using threshold collision-induced dissociation (CID) measurements. The rationale in adopting this combined approach was that (1) few silver binding energies exist for us to verify the accuracy of either the DFT or threshold CID approach; and (2) threshold CID experiments are typically performed on specially constructed mass spectrometers.<sup>16–23</sup>

The silver (I) ion has 46 electrons with a closed shell structure of 4s<sup>2</sup> 4p<sup>6</sup> 4d<sup>10</sup>; few basis sets have been optimized for this element. The study on Ag<sup>+</sup> binding to acetone and unsaturated hydrocarbons<sup>14</sup> employed the silver basis set developed by Langhoff,<sup>25</sup> which combines the relativistic effective core potential of Hay and Wadt<sup>26</sup> with a (6s6p5d3f)/[5s4p4d1f] set describing the valence shell plus polarization functions. The work on Ag<sup>+</sup> binding to a number of small ligands<sup>15</sup> employed also the relativistic effective core potential of Hay and Wadt<sup>26</sup> plus a double-zeta valence basis set for Ag<sup>+</sup>, and the 3-21G(d) basis set for the ligand for geometric optimization at the MP2 level of theory. Single-point calculations at the CCSD(T) level of theory were then employed, again with the Hay and Wadt set for Ag<sup>+</sup> and a 6-31G basis set for the ligand. The silver-ammonia binding study<sup>16</sup> used the double-zeta-valence-polarization (DZVP) basis set<sup>27,28</sup> developed for DFT. Using the DFT hybrid method, B3LYP,<sup>29–31</sup> Shoeib et al.<sup>16</sup> demonstrated that, at least for Mg(NH<sub>3</sub>)<sub>*n*</sub><sup>+</sup> complexes, the DZVP basis set produces energies and structures that are comparable to those obtained using the better-tested basis set, 6-31+G(d).<sup>32–35</sup> For Ag-(NH<sub>3</sub>)<sub>*n*</sub><sup>+</sup> complexes, the binding energies calculated using B3LYP/DZVP agreed well with published experimental val-

\* To whom correspondence should be addressed. Tel: (416) 650-8021. Fax: (416) 736-5936. E-mail: kwmsiu@yorku.ca, siadftcidpa4.

ues.<sup>12</sup> Both the B3LYP/DZVP and the HF/LANL2DZ (a basis set that combines the Hay and Wadt<sup>26</sup> relativistic effective core potential with a double-zeta description of the valence space) approaches were found to yield comparable structures and energetics for the silver(I)-glycine complex.<sup>10</sup> Furthermore, in a recent study the binding energies of acetonitrile to  $\text{Ag}(\text{NCCH}_3)_n^+$  ( $n = 0$  and 1) calculated using B3LYP/DZVP were found to be virtually identical to experimental energies.<sup>36</sup> In addition, the DZVP basis set has also been found to be reliable in determining the structures and energetics of protonated and methylated species, including those of the relatively heavy atoms, Kr and Xe.<sup>37</sup> Thus, there is evidence from the few studies that are available to allow one to be guardedly optimistic that accurate  $\text{Ag}^+$  binding energies can be calculated using B3LYP/DZVP.

One of the most effective ways to measure metal ion-ligand binding energies is threshold collision-induced dissociation.<sup>17–24</sup> Under single-collision conditions, the threshold energy required to dissociate the  $\text{Ag}^+\text{-L}$  complex into  $\text{Ag}^+$  and L is the binding energy of  $\text{Ag}^+$ , provided that the observation window for the dissociation is sufficiently wide, relative to the lifetime of the collisionally activated complex, to render the kinetic shift negligible.<sup>17–23</sup> For complexes whose lifetimes are sufficiently long for the kinetic shift to be sizable, the effect of the kinetic shift must be subtracted from the apparent threshold energy.<sup>22,23</sup> Threshold CID measurements have traditionally been measured on guided ion beam tandem mass spectrometers specially constructed for the purpose.<sup>17–23,38</sup> In recent years, they have also been successfully implemented on similar, commercially available tandem mass spectrometers for electrospray-generated ions.<sup>36,39–42</sup> In this study, threshold CID binding energies of  $\text{Ag}^+$  were measured on one of these tandem mass spectrometers.

### Computational Methods

DFT calculations employing the hybrid B3LYP method (using Becke's three-parameter exchange functional<sup>29,30</sup> and the correlation functional from Lee, Yang, and Parr<sup>31</sup>) with the DZVP basis set<sup>27,28</sup> in Gaussian 98<sup>43</sup> have been used to calculate the optimized geometries, energetics, and vibrational frequencies of the ligands and their silver (I) complexes. All structures were characterized to be at minima by harmonic frequency calculations.

The binding energy between  $\text{Ag}^+$  and a ligand, L, the standard enthalpy change of the reaction,  $\text{Ag}^+\text{-L} \rightarrow \text{Ag}^+ + \text{L}$ , at 0 K,  $\Delta H^\circ_0$ , was calculated as follows

$$\Delta H^\circ_0 = \Delta E_{\text{elec}} + \Delta E_{\text{ZPVE}} \quad (2)$$

where  $\Delta E_{\text{elec}}$  and  $\Delta E_{\text{ZPVE}}$  are the changes in electronic energies and zero-point vibrational energies, respectively, between the products and the reactant in the dissociation reaction.

Basis set superposition errors (BSSE) were calculated using the full counterpoise correction procedure.<sup>44</sup>

### Experimental Method and Data Treatment

**Mass Spectrometric Hardware.** Threshold CID measurements were conducted on a PE SCIEX API III triple-quadrupole mass spectrometer (Concord, Ontario). The samples were typically 50  $\mu\text{M}$  in ligand and 30  $\mu\text{M}$  in silver nitrate in a solution of 50/50 water/methanol. The sample solution was introduced into the ion source at atmospheric pressure using a syringe pump (Harvard Apparatus, Model 22, South Natick, MA) at a typical flow rate of 2  $\mu\text{L}/\text{min}$  and ionized by means of pneumatically assisted electrospray with air being the

nebulizer gas. The optimum electrospray probe position was established from time to time, but was typically with the tip about 2 cm from the interface plate and with the spray off-axis from the orifice. The ions were sampled from the atmospheric-pressure ion source into an "enclosed" quadrupolar lens region (q0) where multiple collisions with the 'curtain-gas' molecules (nitrogen) sampled along with the ions take place. The bias potentials in this lens region were set up to strike a compromise between adequate transmission and minimal collisional heating of the silver-ligand complex. Extensive studies have shown that thermalization of the sampled ions is highly efficient in the lens region (from the orifice to q0 in our mass spectrometer).<sup>45–52</sup> Mass analysis of the ions was performed at unit-mass resolution at a step size of 0.1 Th and at a dwell time of 50 ms/step. Collision-induced dissociation was performed with argon or xenon as the neutral gas. The gas pressure in q2 was continuously monitored with an upstream baratron gauge, the read out of which was converted into collision-gas thickness (CGT)<sup>53</sup> by the mass spectrometric software. (CGT is the product of the neutral gas number density and the length of q2.)

**Determination of the Threshold CID Energies.** The threshold energy for the collision-induced dissociation of a given  $\text{Ag}^+\text{-L}$  complex was determined using the curve-fitting and modeling program, CRUNCH, developed by Armentrout and co-workers<sup>17–23</sup>

$$\sigma(E) = \sigma_0 \sum g_i (E + E_i - E_0)^n / E \quad (3)$$

where  $\sigma(E)$  is the dissociation cross-section,  $\sigma_0$  is a scaling factor,  $E$  is the center-of-mass collision energy ( $E_{\text{cm}}$ ),  $E_0$  is the threshold energy,  $E_i$  is the internal energy of a given vibrational state with a relative population of  $g_i$ , and  $n$  is an adjustable parameter.

An inherent assumption in the use of Equation 3 is that a precursor ion with an internal energy greater than  $E_0$  will fragment to form the product ions in q2. With increasing complexity of the precursor ion, there is an increasing probability that the fragmentation reaction would not occur within the precursor ion's residence time in q2. For a relatively large precursor ion (having many degrees of freedom), additional internal energy may be needed to ensure that the fragmentation rate is sufficiently high for the dissociation to be observable within q2. This additional internal energy, the kinetic shift, must be subtracted from the apparent threshold to yield the true  $E_0$ . The magnitude of the kinetic shift can be estimated from the unimolecular rate constant of the dissociation according to the Rice–Ramsperger–Kassel–Marcus (RRKM) theory.<sup>54–56</sup> When this is done, Equation 3 is modified to become

$$\sigma(E) = \sigma_0 \sum g_i P(E, E_i, t) (E + E_i - E_0)^n / E \quad (4)$$

where  $P$  is the probability that a precursor ion of collision energy  $E$  and internal energy  $E_i$  will fragment within a residence time of  $t$ .

The residence time of a given precursor ion is estimated according to Klassen and Kebarle.<sup>41</sup> In our apparatus, ion residence times for the  $\text{Ag}^+\text{-L}$  complexes of the five oxygen-containing ligands were found to range from 28 to 34  $\mu\text{s}$ , a range very similar to that reported by Kebarle and co-workers.<sup>40,41</sup>

Determination of  $E_0$  requires the vibrational frequencies and rotational constants of the precursor ions and the transition states. The transition states were assumed to be loose and product-like (the phase-space limit, PSL) and their vibrational frequencies are approximated by those of the neutral products obtained

in the DFT calculations (Table 2s). The vibrational modes of the precursor ion that became rotations of the completely dissociated products were treated as rotors. The transition state was assumed to be variationally located at the centrifugal barrier and the adiabatic 2D rotational energy was calculated using the statistical average approach detailed by Rodgers et al.<sup>22</sup> In the Results and Discussion it will be shown that the  $E_0$  obtained both with and without the kinetic shift consideration are comparable (i.e., the kinetic shifts are insignificant) except for those of the largest ligand, diethyl ether, thus rendering details of the choice of the transition states and vibrational frequencies relatively unimportant.

The dissociation cross sections of the product ion,  $\text{Ag}^+$ , were determined as a function of the center-of-mass collision energies at four neutral gas (typically Ar) pressures, expressed as CGT units, and typically = 100, 70, 50, and  $30 \times 10^{12}$  atoms  $\text{cm}^{-2}$ . For an ion that has a collision cross section of  $100 \text{ \AA}^2$ , it will have on average one collision in  $q_2$  with a neutral gas molecule having a CGT value of  $100 \times 10^{12}$  atoms  $\text{cm}^{-2}$ . To eliminate the effects of multiple collisions,  $E_0$  values were obtained from threshold curves constructed only from  $\sigma(E)$  at zero CGT (pressure). These cross sections were obtained by extrapolating the  $\sigma(E)$  versus CGT function to zero CGT via the least-squares fit of the presumed exponential function (vide infra). Typically a threshold curve comprises 120  $\sigma(E)$  values over an  $E_{\text{cm}}$  range of 0–4 eV.

The effects of the ion energy distribution<sup>57</sup> and the thermal motion of the target gas<sup>57,58</sup> on  $\sigma(E)$  were taken into account.<sup>17,59</sup> A target gas temperature gradient likely exists in our mass spectrometer, as its vacuum is maintained by cryopumping. Thus target gas molecules that are closer to the periphery of  $q_2$  are likely to be cooler than those near the axis. As accurate temperature measurements are very difficult to implement, we have opted to assess the effects of the target gas thermal motion by determining the binding enthalpies using two possible extreme target temperatures, 20 K (the temperature adjacent to the cryosurface) and 298 K. Binding enthalpies were determined at minimum in triplicates; the uncertainty in these repeat analyses was comparable to the difference in the means determined for these two target gas temperatures. As a result, all binding enthalpies reported in this study are averages of, and the uncertainties the combined uncertainties (2–4 kcal/mol) of, the two temperature data sets (vide infra). The kinetic energy distributions of the ions entering  $q_2$  were estimated by performing the following stopping potential experiments. The quadrupole lens,  $q_0$ , was typically biased to 40 V; the first quadrupole to 39.9 V; the potential applied to  $q_2$  was decreased from 45 to 35 V. The first-derivative plots of the relative abundance versus the difference in bias potentials between  $q_0$  and  $q_2$  (two examples are shown in Figure 1s of the Supplementary Information Section) show typical full-width-at-half-maximum values of approximately 2 V, thus translating to center-of-mass energy distributions of approximately 0.3–0.5 eV in the threshold CID experiments, which were factored in the determination of  $\sigma(E)$ . These kinetic energy distributions are comparable to the best results obtained in earlier studies on electrospray-generated ions using an older version of our apparatus.<sup>39–41</sup>

The ion temperature is a reflection of  $E_i$ . It has been generally assumed that ions sampled under low-field conditions in apparatus such as ours would have a temperature close to that of ambient.<sup>39,45</sup> In this study, we are assuming an ion temperature of 298 K; the ions were generated at room temperature and that at the end of the free jet the ion temperature would be

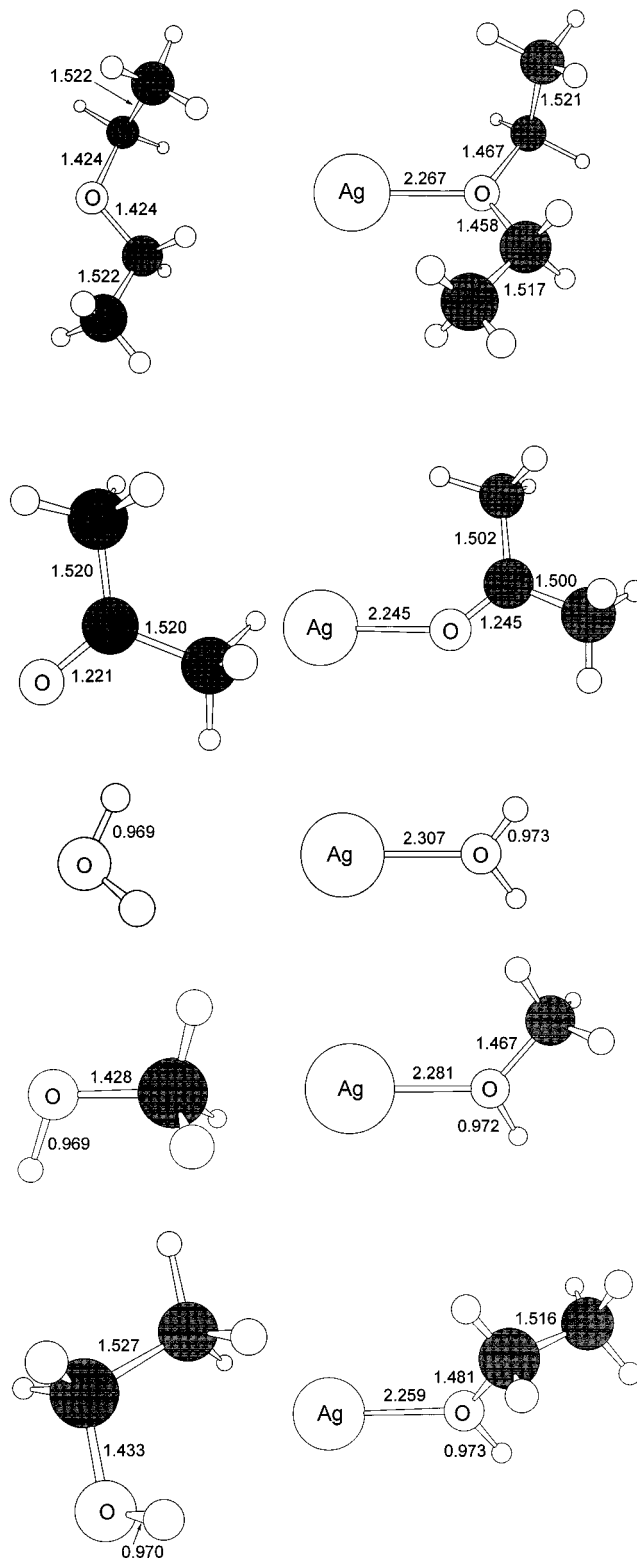


**Figure 1.** Most stable structures of the ligands and the silver complexes: gray circle, carbon; open circle, hydrogen; oxygen and silver atoms are labeled; bond distances in Å.

approximately room temperature.<sup>51</sup> This degree of uncertainty is acceptable as the exact value of the ion temperature is noncrucial in the data analysis. In fact, the ion temperature can vary over a wide range for the determined  $E_0$  values to stay within their experimental uncertainties. For  $\text{Ag}^+ - \text{H}_2\text{O}$ , having the ion temperature range from 85 to 565 K produces an  $E_0$  error that matches the 0.11 eV uncertainty in the  $E_0$  measurements. For  $\text{Ag}^+ - \text{diethyl ether}$ , an ion temperature range of 210–

**TABLE 1: Binding Energies of Na<sup>+</sup> to Water, Methanol, and Ethanol at 0 K (kcal/mol)<sup>a</sup>**

ligand	water	methanol	ethanol
this study			
threshold CID	24.7 ± 1.8	26.1 ± 2.7	28.1 ± 2.0
MP4 <sup>b</sup>	22.8	24.1	26.4
CCSD(t) <sup>c</sup>	22.9	24.2	25.8
CCSD(t) <sup>d</sup>	22.7	25.0	25.5
B3LYP <sup>e</sup>	24.9	26.1	27.6
Rodgers and Armentrout <sup>60</sup>			
threshold CID	22.6 ± 1.8	21.9 ± 1.4	24.4 ± 0.9
CBS-Q	21.2	23.0	25.0
G3	23.5	26.1	28.9
Guo et al. <sup>61</sup>		26.6 ± 0.2	
Hoyau et al. <sup>62</sup>	21.3	23.7 ± 0.2	
Marinelli and Squires <sup>24</sup>	20.2 ± 4		
Dzidic and Kebarle <sup>63</sup>	23.2		
Burdett et al. <sup>64</sup>	23.3 ± 2		

<sup>a</sup> Literature values not at 0 K have been converted to that temperature.

<sup>b</sup> MP4SDTQ(fc)/6-311++G(2df,p)//MP2(fu)/6-311++G(d,p). <sup>c</sup> CCSD(t)(fc)/6-311++G(2df,p)//MP2(fu)/6-311++G(d,p). <sup>d</sup> CCSD(t)(fc)/6-311++G(2df,p)//B3LYP/6-311++G(d,p). <sup>e</sup> B3LYP/DZVP//B3LYP/DZVP.

364 K matches the smaller 0.07 eV uncertainty in the  $E_0$  measurements.

**Validation.** The performance of our mass spectrometer for threshold CID measurements was evaluated and found to be satisfactory in an exercise of measuring the binding energies of Na<sup>+</sup> to water, methanol and ethanol.

Table 1 summarizes the results of this validation exercise. There is acceptable to good agreement between our data and literature data, which have recently been reviewed and evaluated.<sup>60</sup> Our experimental values are in good agreement with our calculated values and the G3 values of Rodgers and Armentrout.<sup>60</sup> We have shown that calculations performed at the levels of MP4 and CCSD(t) using large basis sets, such as 6-311++G(2df,p), are typically within 3 kcal/mol from the best experimental results.<sup>65,66</sup> For the Na<sup>+</sup>-methanol and Na<sup>+</sup>-ethanol binding energies measured by threshold CID, the sets differ by approximately 4 kcal/mol, which is comparable to the sum of the uncertainties of the two measurements. There are too few data points to allow one to comment on whether this reveals a systematic difference between the two experimental sets of data.

## Results and Discussion

**DFT Structures and Energetics.** The optimum structures of the ligands and their Ag<sup>+</sup> complexes are illustrated in Figure 1. The electronic energies, zero-point vibrational energies, enthalpy corrections required to convert from 0 to 298 K, and entropies of water, methanol, ethanol, diethyl ether, and acetone and their Ag<sup>+</sup> complexes are shown in Table 1s of the Supplementary Information Section. The vibrational frequencies and rotational constants of the ligands and the complexes used in the  $E_0$  determinations are listed in Table 2s of the same Section. For every complex, Ag<sup>+</sup> binding occurs on the oxygen atom; there is a small increase of the O–C bond distance (by 0.02–0.05 Å) upon argentination, otherwise the structures of the ligands remain essentially unchanged. The Ag<sup>+</sup>–O bond distance increases from a minimum of 2.245 Å in the Ag<sup>+</sup>-acetone complex to a maximum of 2.307 Å in the Ag<sup>+</sup>-water complex. In general, the order of increasing Ag<sup>+</sup>–O bond distances is in keeping with the order of decreasing silver binding energies, a reflection of the similarity in ligand structures between their free and silver-bound states.

The  $\Delta H^{\circ}_0$  as deduced from the differences in electronic energies and zero-point vibrational energies for the dissociation

**TABLE 2: Enthalpies for Reactions Ag<sup>+</sup>-L → Ag<sup>+</sup> + L<sup>a</sup>**

L	$\Delta H^{\circ}_0$	BSSE	$\Delta H^{\circ}_{0(\text{corr})}$ <sup>b</sup>
water	29.1	1.0	28.1
methanol	31.1	1.0	30.1
ethanol	33.1	1.1	32.0
diethyl ether	34.9	1.6	33.3
acetone	37.4	1.2	36.2

<sup>a</sup> All values are in kcal/mol. <sup>b</sup> Corrected for BSSE.

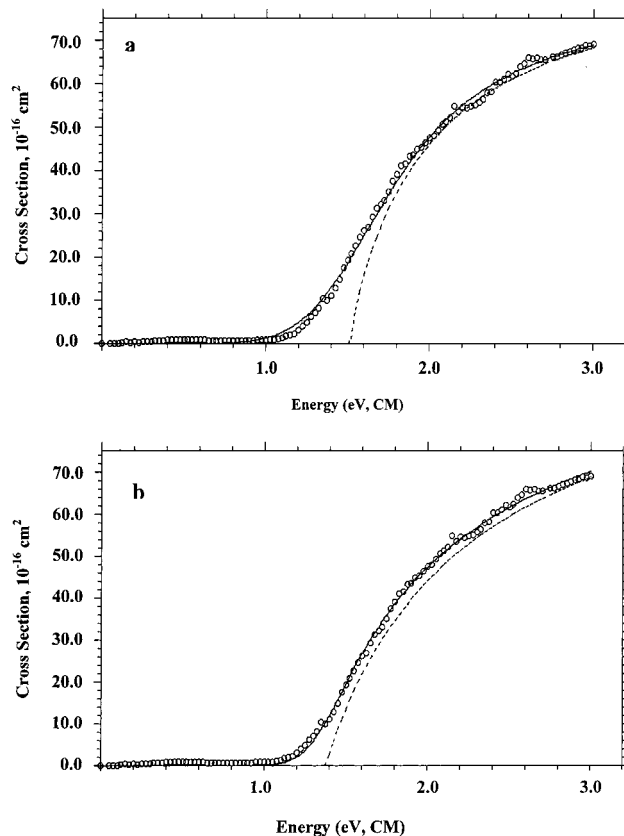


**Figure 2.** Zero CGT threshold curve for Ag<sup>+</sup>-water: open circles, experimental data; solid line, best fit to the experimental data; dashed line, modeled cross section at 0 K; Ar temperature of (a) 298 K and (b) 20 K.

reaction Ag<sup>+</sup>-L → Ag<sup>+</sup> + L are shown in Table 2. The basis set superposition errors and the  $\Delta H^{\circ}_0$  incorporating this correction are also listed. The silver(I) binding energies range from a low of 28.1 kcal/mol for water to a high of 36.2 kcal/mol for acetone. For saturated ligands such as water, methanol and ethanol, the Ag<sup>+</sup> binding energies increase with the size of the ligands. They are lower than the corresponding Li<sup>+</sup> binding energies,<sup>59,67,68</sup> but are higher than the Na<sup>+</sup> binding energies (vide infra).<sup>24,60–64</sup>

**Threshold CID Measurements.** Figure 2 shows a typical threshold curve for Ag<sup>+</sup>-H<sub>2</sub>O at zero CGT. The experimental dissociation cross sections (the open circles) are near zero for low  $E_{\text{cm}}$  values. They start to increase beyond a certain critical  $E_{\text{cm}}$  value, approximately 1.1 eV. The increase slows down between 2 and 3 eV and reaches a plateau beyond 3 eV (not shown). The solid line is the best fit to the experimental data. The dashed line shows the modeled cross sections at 0 K and gives an  $E_0$  at (a) 1.50 eV (Ar temperature of 298 K) and (b) 1.37 eV (Ar temperature of 20 K).

As described earlier,  $\sigma(E)$  at zero CGT were obtained by extrapolating the measured  $\sigma(E)$  at CGT values of typically 30, 50, 70 and 100 × 10<sup>12</sup> atoms cm<sup>-2</sup> to zero CGT. Figure 3 shows the dependence of cross sections on CGT at two  $E_{\text{cm}}$  values,

### Extrapolation to zero CGT<sup>†</sup> (Silver- Water)

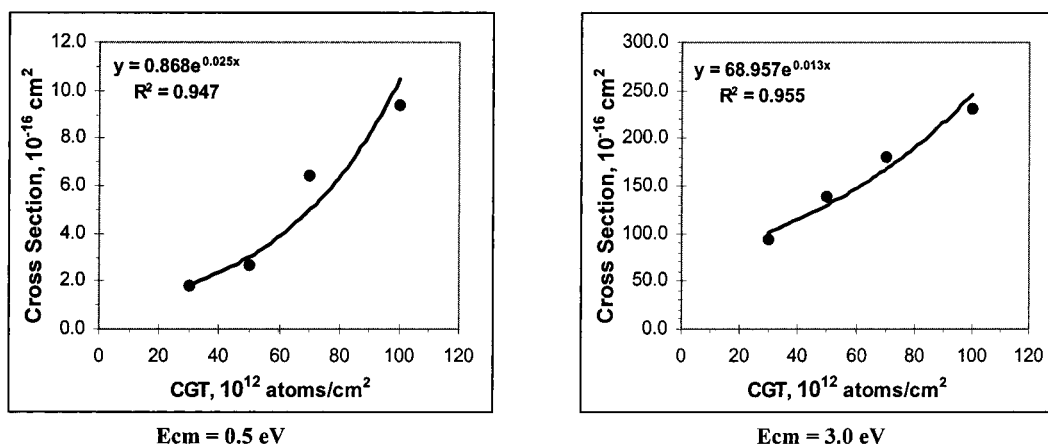


**Figure 3.** Dependence of cross sections on collision-gas thickness:  $E_{\text{cm}}$  values of 0.5 and 3.0 eV. ●, experimental data; line, best exponential fit to the data. The cross section values obtained at zero CGT are  $0.859$  and  $68.96 \times 10^{-16} \text{ cm}^2$ , respectively.

**TABLE 3: Binding Energies of  $\text{Ag}^+$  to Ligands (eV)**

L	$E_0$	$E_0$ (PSL)	$\Delta S^\ddagger$ (PSL) <sup>a</sup>
water	$1.37 \pm 0.11^b$	$1.37 \pm 0.11$	1.80
methanol	$1.44 \pm 0.16$	$1.43 \pm 0.16$	2.03
ethanol	$1.50 \pm 0.16$	$1.47 \pm 0.15$	4.16
diethyl ether	$1.62 \pm 0.10$	$1.44 \pm 0.07$	6.25
acetone	$1.70 \pm 0.07$	$1.65 \pm 0.06$	8.83

<sup>a</sup> Entropy of activation at 1000 K, in cal/(K mol). <sup>b</sup> Standard deviation;  $n$  (number of replicate analyses) = 3, except for diethyl ether where  $n = 4$ .

0.5 and 3.0 eV; the plots of intermediate energies are similar.  $\sigma(E)$  is evidently a nonlinear function of CGT; the choice of using four CGT values is a compromise between time and accuracy.

Argon and xenon performed equally well as the collision gas. The threshold curves for a given complex at the full range of CGT were very similar between the two collision partners. In addition, no significant difference was evident between the  $E_0$  determined using the two gases; the relative standard deviations were typically within 5% irrespective of one or both collision gases were being considered.

The  $E_0$  of the five complexes are shown in Table 3. Two types of  $E_0$  data are on display: those obtained without considerations of dissociation rates (i.e., no kinetic shifts are assumed; labeled simply as  $E_0$ ) and those for which kinetic shifts are taken into account (labeled as  $E_0$ (PSL)). The threshold energies are averages of three independent measurements with the exception of those for diethyl ether, which comprises four measurements. The standard deviations of the measurements range from a low of 3.6% for acetone to a high of 11.2% for methanol, with an average of 7.7%. Comparing the  $E_0$  data with and without kinetic shift considerations, it is evident that the shifts are insignificant (<5%) for water, methanol, ethanol, and acetone. For diethyl ether, the largest ligand under consideration, the kinetic shift is approximately 11% of the  $E_0$  without ion lifetime considerations. This means that even for the  $\text{Ag}^+$ -diethyl ether complex, minor inaccuracies in the choice of the type of transition state structures, vibrational frequencies and residence times are inconsequential.

The  $\text{Ag}^+$  binding energies as determined using DFT and threshold CID are compared in Table 4. The experimental binding enthalpies are those converted from the threshold values listed in the  $E_0$  (PSL) column of Table 3. It is gratifying that

**TABLE 4: Calculated and Experimental  $\text{Ag}^+$  Binding Enthalpies at 0 K (kcal/mol)**

L	DFT	threshold CID	$\Delta H_{298}^\circ - \Delta H_0^\circ$ <sup>a</sup>	literature
water	28.1	$31.6 \pm 2.5$	0.7	$32.6 \pm 2.2^b/29.4^c$
methanol	30.1	$33.0 \pm 3.7$	0.3	$33.9^c$
ethanol	32.0	$33.9 \pm 3.5$	0.3	
diethyl ether	33.3	$33.2 \pm 1.5$	0.2	
acetone	36.2	$38.0 \pm 1.4$	0.3	$38.5^c/38.3 \pm 4.6^d$

<sup>a</sup> Thermal correction for interconverting between 0 and 298 K data, from B3LYP/DZVP calculations. <sup>b</sup> Reference 12, converted from 298 K data. <sup>c</sup> Reference 15. <sup>d</sup> Reference 14.

the binding energies obtained via the two approaches are comparable, the average of the absolute differences being 2.0 kcal/mol, a value within experimental uncertainties (average of 2.6 kcal/mol) and expected accuracies of DFT calculations. The good agreement between the two sets of data is in direct support of the reliability of both the DFT and the threshold CID approaches. For the binding enthalpies of water, methanol, and acetone (for which comparisons are possible), there is good agreement between our data and literature data.

The correlations between the silver, lithium, and sodium binding energies are shown in Figure 4. It is evident that binding energies increase with the degree of substitution in the alcohols (water, methanol, and ethanol) and that the silver ion binding energies are smaller than their corresponding lithium ion binding energies, but larger than the sodium ion binding energies. The interaction between the metal ion and the ligand is predominantly electrostatic.<sup>59,69</sup> The increase in binding energy with substitution has been attributed to increasing ion-induced dipole interaction in the complexes,<sup>59</sup> which is a consequence of increasing polarizability from water ( $1.45 \times 10^{-24} \text{ cm}^3$ ) to methanol ( $3.29 \times 10^{-24} \text{ cm}^3$ ) to ethanol ( $5.41 \times 10^{-24} \text{ cm}^3$ ).<sup>70</sup> The decrease in binding energy from  $\text{Li}^+$  to  $\text{Na}^+$  is due to an increase in ion size, which decreases the metal ion–ligand interaction because of increased bond distance.<sup>59</sup> The silver ion is even larger than the sodium ion; its relatively large binding energies have been attributed to  $sd\sigma$  hybridization which reduces electron–electron repulsion by lessening electron density in the Ag–O axis.<sup>20,59</sup>

**Acknowledgment.** We thank Professor P. B. Armentrout for making his CRUNCH program available to us. We would also like to thank him, Professor M. T. Rodgers and Dr. A. A.

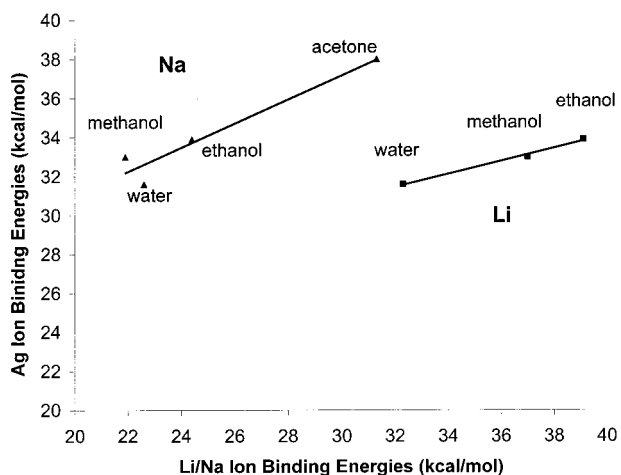


**Figure 4.** Silver ion binding energies versus lithium and sodium ion binding energies: threshold CID Ag ion binding energies are plotted; Li ion binding energies from refs 67 (water) and 68 (methanol and ethanol); and Na ion binding energies from refs 60 (water, methanol and ethanol) and 59 (acetone).

Shvartsburg for helpful discussions. This work was supported by the Canadian Natural Science and Engineering Research Council (NSERC), MDS SCIEIX, the Canadian Foundation of Innovation (CFI), the Ontario Innovation Trust (OIT), and York University. T.S. thanks the Ontario Graduate Scholarship in Science and Technology for financial support.

**Supporting Information Available:** Figure 1s: stopping curves and first-derivative plots of  $\text{Ag}^+$ -water and  $\text{Ag}^+$ -diethyl ether; Table 1s: electronic energies, zero-point vibrational energies, enthalpy corrections for converting from 0 to 298 K, and entropies of the ligands and their  $\text{Ag}^+$  complexes; and Table 2s: vibrational frequencies and rotational constants of the ligands and the complexes. This material is available free of charge via the Internet at <http://pubs.acs.org>.

## References and Notes

- Petering, H. G. *Pharmac. Ther. A* **1976**, *1*, 127–130.
- Wigley, R. A.; Brooks, R. R. In *Noble Metals and Biological Systems*; Brooks, R. R., Ed.; CRC Press: Boca Raton, FL, 1992; pp 277–297.
- Nomiya, K.; Onoue, K. I.; Kondoh, Y.; Kasuga, N. C.; Nagano, H.; Oda, M.; Sakuma, S. *Polyhedron* **1995**, *14*, 1359–1367.
- Nomiya, K.; Kondoh, Y.; Nagano, H.; Oda, M. *J. Chem. Soc. Chem. Commun.* **1995**, 1679–1680.
- Narula, S. S.; Mehra, R. K.; Winge, D. R.; Armitage, I. M. *J. Am. Chem. Soc.* **1991**, *113*, 9354–9358.
- Stillman, M. J.; Presta, A.; Gui, Z.; Jiang, D.-T. In *Metal-Based Drugs*; Gielen, M., Ed.; Freund: London, 1994; Vol. 1, pp 375–393.
- Gui, Z.; Green, A. R.; Kasrai, M.; Bancroft, G. M.; Stillman, M. J. *Inorg. Chem.* **1996**, *35*, 6520–6529.
- Li, H.; Siu, K. W. M.; Guevremont, R.; Le Blanc, J. C. Y. *J. Am. Soc. Mass Spectrom.* **1997**, *8*, 781–792.
- Lee, V. W.-M.; Li, H.; Lau, T.-C.; Siu, K. W. M. *J. Am. Chem. Soc.* **1998**, *120*, 7302–7309.
- Chu, I. K.; Shoeib, T.; Guo, X.; Rodriguez, C. F.; Lau, T.-C.; Hopkinson, A. C.; Siu, K. W. M. *J. Am. Soc. Mass Spectrom.* **2001**, *12*, 163–175.
- Chu, I. K.; Guo, X.; Lau, T.-C.; Siu, K. W. M. *Anal. Chem.* **1999**, *71*, 2364–2372.
- Holland, P. M.; Castleman, A. W., Jr. *J. Chem. Phys.* **1982**, *76*, 4195–4205.
- Deng, H.; Kebarle, P. *J. Phys. Chem. A* **1998**, *102*, 571–579.
- Ho, Y.-P.; Yang, Y.-C.; Klippenstein, S. J.; Dunbar, R. C. *J. Phys. Chem. A* **1997**, *101*, 3338–3347.
- Ma, N. L. *Chem. Phys. Lett.* **1998**, *297*, 230–238.
- Shoeib, T.; Millburn, R. K.; Koyanagi, G. K.; Lavrov, V. V.; Bohme, D. K.; Siu, K. W. M.; Hopkinson, A. C. *Int. J. Mass Spectrom.* **2000**, *201*, 87–100.
- Ervin, K. M.; Armentrout, P. B. *J. Chem. Phys.* **1985**, *83*, 166–189.
- Weber, M. E.; Elkind, J. L.; Armentrout, P. B. *J. Chem. Phys.* **1986**, *84*, 1521–1529.
- Schultz, R. H.; Crellin, K. C.; Armentrout, P. B. *J. Am. Chem. Soc.* **1991**, *113*, 8590–8601.
- Dalleska, N. F.; Honma, K.; Sunderlin, L. S.; Armentrout, P. B. *J. Am. Chem. Soc.* **1994**, *116*, 3519–3528.
- Shvartsburg, A. A.; Ervin, K. M.; Frederick, J. H.; *J. Chem. Phys.* **1996**, *104*, 8458–8469.
- Rodgers, M. T.; Ervin, K. M.; Armentrout, P. B. *J. Chem. Phys.* **1997**, *106*, 4499–4508.
- Rodgers, M. T.; Armentrout, P. B. *J. Chem. Phys.* **1998**, *109*, 1787–1800.
- Marinelli, P. J.; Squires, R. R. *J. Am. Chem. Soc.* **1989**, *111*, 4101–4103.
- Langhoff, S. R.; Pettersson, L. G. M.; Bauschlicher, C. W.; Partridge, H. *J. Chem. Phys.* **1987**, *86*, 268–278.
- Hay, P. J.; Wadt, W. R. *J. Chem. Phys.* **1985**, *82*, 299–310.
- Godbout, N.; Salahub, D. R.; Andzelm, J.; Wimmer, E. *Can. J. Chem.* **1992**, *70*, 560–571.
- Godbout, N. *Ensemble de base pour la théorie de la fonctionnelle de la densité—Structures moléculaires, propriétés mono-électroniques et modèles de zéolites*; Ph. D. dissertation, Département de chimie, Faculté des arts et des sciences, Université de Montréal, 1996.
- Becke, A. D. *Phys. Rev.* **1988**, *A38*, 3098–3100.
- Becke, A. D. *J. Chem. Phys.* **1993**, *98*, 5648–5652.
- Lee, C.; Yang, W.; Parr, R. G. *Phys. Rev.* **1988**, *B37*, 785–789.
- Hariharan, P. C.; Pople, J. A. *Chem. Phys. Lett.* **1972**, *66*, 217.
- Francl, M. M.; Pietro, W. J.; Hehre, W. J.; Binkley, J. S.; Gordon, M. S.; DeFrees, D. J.; Pople, J. A. *J. Chem. Phys.* **1982**, *77*, 3654–3665.
- Chandrasekhar, J.; Andrade, J. G.; Schleyer, P. v. R. *J. Am. Chem. Soc.* **1981**, *103*, 5609.
- Chandrasekhar, J.; Spitznagel, G. W.; Schleyer, P. v. R. *J. Comput. Chem.* **1983**, *4*, 294.
- Shoeib, T.; El Aribi, H.; Siu, K. W. M.; Hopkinson, A. C. *J. Phys. Chem. A* **2001**, *105*, 710–719.
- Cunje, A. *Catalysis of Intramolecular Rearrangements in the Gas Phase*; Ph. D. dissertation, Department of Chemistry, Faculty of Pure and Applied Science, York University, 2000.
- Bell, R. C.; Zemski, K. A.; Justes, D. R.; Castleman, A. W., Jr. *J. Chem. Phys.* **2001**, *114*, 798–811.
- Anderson, S. G.; Blades, A. T.; Klassen, J.; Kebarle, P. *Int. J. Mass Spectrom. Ion Processes* **1995**, *141*, 217–228.
- Klassen, J. S.; Anderson, S. G.; Blades, A. T.; Kebarle, P. *J. Phys. Chem.* **1996**, *100*, 14 218–14 227.
- Klassen, J. S.; Kebarle, P. *J. Am. Chem. Soc.* **1997**, *119*, 6552–6563.
- El Aribi, H.; Rodriguez, C. F.; Shoeib, T.; Ling, Y.; Hopkinson, A. C.; Siu, K. W. M. *Proceedings of the 49th American Society for Mass Spectrometry Conference*, Chicago, IL, May 27–31, 2001, A010079.pdf.
- M. J. Frisch, G. W. Trucks, H. B. Schlegel, G. E. Scuseria, M. A. Robb, J. R. Cheeseman, V. G. Zakrzewski, J. A. Montgomery, Jr., R. E. Stratmann, J. C. Burant, S. Dapprich, J. M. Millam, A. D. Daniels, K. N. Rudin, M. C. Strain, O. Farkas, J. Tomasi, V. Barone, M. Cossi, R. Cammi, B. Mennucci, C. Pomelli, C. Adamo, S. Clifford, J. Ochterski, G. A. Petersson, P. Y. Ayala, Q. Cui, K. Morokuma, D. K. Malick, A. D. Rabuck, K. Raghavachari, J. B. Foresman, J. Cioslowski, J. V. Ortiz, B. B. Stefanov, G. Liu, A. Liashenko, P. Piskorz, I. Komaromi, R. Gomperts, R. L. Martin, D. J. Fox, T. Keith, M. A. Al-Laham, C. Y. Peng, A. Nanayakkara, C. Gonzalez, M. Challacombe, P. M. W. Gill, B. Johnson, W. Chen, M. W. Wong, J. L. Andres, C. Gonzalez, M. Head-Gordon, E. S. Replogle and J. A. Pople, *Gaussian 98, Revision A.5*, Gaussian Inc., Pittsburgh, PA, 1998.
- Boys, S. F.; Bernardi, F. *Mol. Phys.* **1970**, *19*, 553.
- Douglas, D. J. *J. Phys. Chem.* **1982**, *86*, 185–191.
- Douglas, D. J.; French, J. B. *J. Am. Soc. Mass Spectrom.* **1992**, *3*, 398–408.
- Covey, T.; Douglas, D. J. *J. Am. Soc. Mass Spectrom.* **1993**, *4*, 616–623.
- Goeringer, D. E.; Asano, K. G.; McLuckey, S. A. *Int. J. Mass Spectrom.* **1999**, *182/183*, 275–288.
- Asano, K. G.; Goeringer, D. E.; McLuckey, S. A. *Int. J. Mass Spectrom.* **1999**, *185/186/187*, 207–219.
- Drahos, L.; Heeren, R. M. A.; Collette, C.; De Pauw, E.; Vékey, K. *J. Mass Spectrom.* **1999**, *34*, 1373–1379.
- Schneider, B. B.; Chen, D. D. Y. *Anal. Chem.* **2000**, *72*, 791–799.
- Schneider, B. B.; Douglas, D. J.; Chen, D. D. Y. *J. Am. Soc. Mass Spectrom.* **2001**, *12*, 772–779.
- Dawson, P. H.; French, J. B.; Buckley, J. A.; Douglas, D. J.; Simmons, D. *Org. Mass Spectrom.* **1982**, *17*, 205–211.
- Gilbert, R. G.; Smith, S. C. *Theory of Unimolecular and Recombination Reactions*; Blackwell Scientific Publications: Oxford, 1990.

- (55) Truhlar, D. G.; Garrett, B. C.; Klippenstein, S. J. *J. Phys. Chem.* **1996**, *100*, 12 771–12 800.
- (56) Holbrook, K. A.; Pilling, M. J.; Robertson, S. H. *Unimolecular Reactions*, 2nd Edition: Wiley: New York, 1996.
- (57) Lifshitz, C.; Wu, R. L. C.; Tiernan, T. O.; Terwilliger, D. T. *J. Chem. Phys.* **1978**, *68*, 247–260.
- (58) Chantry, P. J. *J. Chem. Phys.* **1971**, *55*, 2746–2759.
- (59) Rodgers, M. T.; Armentrout, P. B. *Mass Spectrom. Rev.* **2000**, *19*, 215–247.
- (60) Armentrout, P. B.; Rodgers, M. T. *J. Phys. Chem. A* **2000**, *104*, 2238–2247.
- (61) Guo, B. C.; Conklin, B. J.; Castleman, A. W., Jr. *J. Am. Chem. Soc.* **1989**, *111*, 6506–6510.
- (62) Hoyau, S.; Norrman, K.; McMahon, T. B.; Ohanessian, G. *J. Am. Chem. Soc.* **1999**, *121*, 8864–8875.
- (63) Dzidic, I.; Kebarle, P. *J. Phys. Chem.* **1970**, *74*, 1466–1474.
- (64) Burdett, N. A.; Hayhurst, A. N. *J. Chem. Soc., Faraday Trans. 1* **1982**, *78*, 2997–3007.
- (65) Ketvirtis, A. E.; Bohme, D. K.; Hopkinson, A. C. *J. Phys. Chem.* **1995**, *99*, 16 121–16 127.
- (66) Rodriguez, C. F.; Bohme, D. K.; Hopkinson, A. C. *J. Phys. Chem.* **1996**, *100*, 2942–2949.
- (67) Rodgers, M. T.; Armentrout, P. B. *J. Phys. Chem. A* **1997**, *101*, 1238–1249.
- (68) Rodgers, M. T.; Armentrout, P. B. *J. Phys. Chem. A* **1997**, *101*, 2614–2625.
- (69) Shoeib, T.; Gorelsky, S. I.; Lever, A. B. P.; Siu, K. W. M.; Hopkinson, A. C. *Inorg. Chim. Acta* **2001**, *315*, 236–239.
- (70) Lide, D. R. (Ed) In *CRC Handbook of Chemistry and Physics*, 82nd ed.; CRC Press: Boca Raton, 2001, pp 10–162 to 10–174.